Journal of Mathematical Modeling
Vol. 10, No. 4, 2022, pp. 555-567. Research Article

JMM

WENO schemes with Z-type non-linear weighting procedure for fractional differential equations

Rooholah Abedian

School of Engineering Science, College of Engineering, University of Tehran, Iran
Email(s): rabedian@ut.ac.ir

Abstract. In this paper, a new fourth-order finite difference weighted essentially non-oscillatory (WENO) scheme is developed for the fractional differential equations which may contain non-smooth solutions at a later time, even if the initial solution is smooth enough. A set of Z-type non-linear weights is constructed based on the L_1 norm, yielding improved WENO scheme with more accurate resolution. The Caputo fractional derivative of order α is split into a weakly singular integral and a classical second derivative. The classical Gauss-Jacobi quadrature is employed for solving the weakly singular integral. Also, a new WENO-type reconstruction methodology for approximating the second derivative is developed. Some benchmark examples are prepared to illustrate the efficiency, robustness, and good performance of this new finite difference WENO-Z scheme.

Keywords: Finite difference scheme, fractional differential equations, WENO-Z scheme.
AMS Subject Classification 2010: 35R11, 65M06.

1 Introduction

In this research work, a new fourth-order finite difference weighted essentially non-oscillatory (WENO) scheme is developed for solving the fractional differential equations. In recent decades, high-order essentially non-oscillatory (ENO) and WENO methods have been widely considered to solve the hyperbolic conservation laws and approximate the convection terms in convection dominated convection-diffusion partial differential equations, because these methodologies have good properties such as conservation, high-order accuracy in smooth regions, and non-oscillatory near discontinuities.

In 1987, finite volume ENO schemes were developed to solve one-dimensional hyperbolic conservation laws problem [10]. The main objective of these high-order methods was to employ the smoothest spatial stencil among all candidate stencils to obtain numerical approximation at the half points to keep optimal order of accuracy in smooth regions and suppress non-physical oscillations in non-smooth regions. To solve multi-dimensional problems, the finite difference ENO schemes are very simple and efficient which the first version of these schemes are developed by Shu and Osher in [19, 20]. Liu et al. designed a third-order accurate finite volume WENO scheme in [14]. Also, by designing the new

smoothness indicators and non-linear weights, Jiang and Shu [11] proposed a fifth-order finite difference WENO scheme.

More recently, high-order numerical methods for the fractional diffusion equations have attracted a lot of attention. In [15], Liu et al. developed the finite difference WENO schemes for partial differential equations, which approximate the second derivative term directly by a conservative flux difference. However, unlike the positive linear weights of WENO schemes for hyperbolic conservation laws [11], the negative linear weights exist so that some special care, such as the technique in [18], was applied to guarantee the non-oscillatory performance in regions of sharp interfaces. Moreover, the mapped non-linear weights were necessary to achieve designed high order accuracy. After that, Abedian et al. [4] extended the central WENO reconstruction to approximate the second derivative to deal with the appearance of the negative ideal weights and the mapped non-linear weights were also applied to maintain the high-order accuracy in smooth regions. They also did a lot of other interesting work to approximate the second derivative in [1–3, 5]. Liu et al. was introduced the method of lines for solving space fractional differential equations [13]. In [16], Meerschaert and Tadjeran proposed the finite difference scheme for solving space fractional differential equations. Deng developed the finite element scheme for space and time-space fractional differential equations [6]. The spectral method for solving time-space fractional diffusion equations was developed in [12]. Deng et al. extended the high-order finite difference WENO scheme for solving the fractional differential equations, whose solution may be discontinuous [7]. In 2021, Zhang et al. [21] proposed a sixth-order finite difference WENO scheme for solving the fractional differential equations. The aim of this paper is to develop a fourth-order finite difference WENO scheme with Z-type non-linear weighting procedure for solving fractional differential equations containing non-smooth solutions, because there are not many papers on numerically solving the fractional differential equations with discontinuous solutions.

The organization of this research paper is as follows. In Section 2, a new fourth-order finite difference WENO-Z scheme is developed to solve the fractional differential equations in detail. In Section 3, some benchmark numerical test cases are prepared to show the numerical accuracy and resolution of this new WENO-Z method. Concluding remarks are given in Section 4.

2 Fourth-order finite difference WENO method

The one-dimensional fractional differential equation is considered as follows

$$\frac{\partial u(x,t)}{\partial t} = c_1 {}_a^c D_x^\alpha u(x,t) + c_2 {}_x^c D_b^\alpha u(x,t) + f(x,t), \quad x \in [a,b], \tag{1}$$

where $1 < \alpha < 2$, c_1, c_2 are non-negative constants and $c_1 c_2 \neq 0$. Here, the left and right α-th Caputo fractional derivatives are defined by Podlubny [17] as follows

$$\begin{aligned} {}_a^c D_x^\alpha u(x) &= \frac{1}{\Gamma(2-\alpha)} \int_a^x \frac{u''(\xi)}{(x-\xi)^{\alpha-1}} \mathrm{d}\xi, \\ {}_x^c D_b^\alpha u(x) &= \frac{1}{\Gamma(2-\alpha)} \int_x^b \frac{u''(\xi)}{(\xi-x)^{\alpha-1}} \mathrm{d}\xi. \end{aligned} \tag{2}$$

Now, the fractional derivatives are split into a second derivative and an integral part

$$
\begin{aligned}
{}_a^cD_x^\alpha u(x) &= \begin{cases} \frac{1}{\Gamma(2-\alpha)} \int_a^x \frac{v(\xi)}{(x-\xi)^{\alpha-1}} \mathrm{d}\xi, \\ v = u_{xx}, \end{cases} \\
{}_x^cD_b^\alpha u(x) &= \begin{cases} \frac{1}{\Gamma(2-\alpha)} \int_x^b \frac{v(\xi)}{(\xi-x)^{\alpha-1}} \mathrm{d}\xi, \\ v = u_{xx}. \end{cases}
\end{aligned} \tag{3}
$$

Eq. (1) can be rewritten by simple linear transformation as follows [7]

$$
\begin{aligned}
\frac{\partial u(x,t)}{\partial t} =& \frac{1}{\Gamma(2-\alpha)} \Big(c_1 \big(\frac{x-a}{2}\big)^{2-\alpha} \int_{-1}^{1} \frac{v(\frac{a+x}{2} + \frac{x-a}{2}\eta, t)}{(1-\eta)^{\alpha-1}} \mathrm{d}\eta \\
&+ c_2 \big(\frac{b-x}{2}\big)^{2-\alpha} \int_{-1}^{1} \frac{v(\frac{b+x}{2} + \frac{b-x}{2}\eta, t)}{(1+\eta)^{\alpha-1}} \mathrm{d}\eta \Big) + f(x,t), \\
v(x,t) =& \frac{\partial^2}{\partial x^2} u(x,t).
\end{aligned} \tag{4}
$$

The Gauss-Jacobi quadratures with weight functions $(1-\eta)^{1-\alpha}$ and $(1+\eta)^{1+\alpha}$ are employed to solve the two weakly singular integrals in (4), respectively.

A new WENO-Z reconstruction is needed to do the spatial discretization for $v = u_{xx}$ in the conservation form. The construction procedure is narrated in detail as follows.

First,

$$
v(x,t) = \frac{\partial^2}{\partial x^2} u(x,t) = f(u)_{xx}, \tag{5}
$$

is defined. A uniform mesh x_j with the mesh size $\Delta x = x_{j+1} - x_j$ is considered. The half point and the numerical approximation to the nodal point value are denoted by $x_{j+\frac{1}{2}} = \frac{1}{2}(x_j + x_{j+1})$ and $u_j(t)$, respectively. The semi-discrete finite difference scheme of (5) is considered as

$$
v_j(t) = \frac{\hat{f}_{j+\frac{1}{2}} - \hat{f}_{j-\frac{1}{2}}}{\Delta x^2}. \tag{6}
$$

Here, $v_j(t)$ is the numerical approximation to the nodal point value $v(x_j,t)$ of the exact solution. The term $\hat{f}_{j+\frac{1}{2}} = f(u_{j-s}, \cdots, u_{j+s+1})$, is the numerical flux function. It is designed to satisfy the condition that the flux difference approximates $f(u)_{xx}$ with k-th order accuracy

$$
\frac{\hat{f}_{j+\frac{1}{2}} - \hat{f}_{j-\frac{1}{2}}}{\Delta x^2} = f(u)_{xx}|_{x=x_j} + \mathscr{O}(\Delta x^k). \tag{7}
$$

The WENO-Z reconstruction of the second-order derivative is performed in terms of $h(x)$, which is defined as

$$
f(u(x)) = \frac{1}{\Delta x^2} \int_{x-\frac{\Delta x}{2}}^{x+\frac{\Delta x}{2}} \int_{\chi-\frac{\Delta x}{2}}^{\chi+\frac{\Delta x}{2}} h(\psi) \mathrm{d}\psi \mathrm{d}\chi. \tag{8}
$$

Differentiating both sides twice with respect to x, one obtains

$$
f(u)_{xx} = \frac{1}{\Delta x^2} \big(h(x+\Delta x) - 2h(x) + h(x-\Delta x) \big). \tag{9}
$$

Setting $g(x)$ as $g(x) = h(x+\frac{\Delta x}{2}) - h(x-\frac{\Delta x}{2})$ gives the equation

$$f(u)_{xx}\Big|_{x=x_j} = \frac{g(x_{j+\frac{1}{2}}) - g(x_{j-\frac{1}{2}})}{\Delta x^2}. \tag{10}$$

How to develop numerical flux is our main concern in the following.

Step 1. Choose a four-point spatial stencil and two three-point spatial stencils $T_1 = \{x_{j-1}, \ldots, x_{j+2}\}$, $T_0 = \{x_{j-1}, x_j, x_{j+1}\}$, $T_2 = \{x_j, x_{j+1}, x_{j+2}\}$. By approximating $g(x)$, the numerical schemes are formulated. These approximations of $g(x)$ are shown by $P_r(x)$ with $r = 0,1,2$ and are constructed by employing a polynomial form with undetermined coefficients. First, a polynomial of degree three on T_1, demonstrated by $q(x) = \sum_{i=0}^{3} a_i x^i$, is considered to approximate $h(x)$. Next, substituting $q(x)$ into (8) and integrating, $f(u)$ is computed. Then, using the given point-values of $f(u)$ on T_1, a linear system is generated and the coefficients can be explicitly computed. Finally, $P_1(x)$ is completely determined by

$$P_1(x) = q(x+\frac{\Delta x}{2}) - q(x-\frac{\Delta x}{2}). \tag{11}$$

Similarly, two linear polynomials are obtained to approximate $g(x)$ on two smaller stencils T_0 and T_2. The approximations of $g(x)$ at $x_{j+\frac{1}{2}}$ are given by

$$\begin{aligned}
\hat{f}^{(0)}_{j+\frac{1}{2}} &:= P_0(x_{j+\frac{1}{2}}) = f(u_{j+1}) - f(u_j), \\
\hat{f}^{(1)}_{j+\frac{1}{2}} &:= P_1(x_{j+\frac{1}{2}}) = \frac{1}{12}\Big(f(u_{j-1}) - 15f(u_j) + 15f(u_{j+1}) - f(u_{j+2})\Big), \\
\hat{f}^{(2)}_{j+\frac{1}{2}} &:= P_2(x_{j+\frac{1}{2}}) = f(u_{j+1}) - f(u_j).
\end{aligned} \tag{12}$$

It is only needed to shift each index by -1 to obtain the fluxes $\hat{f}^{(r)}_{j-\frac{1}{2}}$ with $r = 0,1,2$.

Step 2. Set any positive linear (ideal) weights d_0, d_1 and d_2, such that $d_0 + d_1 + d_2 = 1$. The main selection principle of the ideal weights is solely based on the consideration of a balance between accuracy and ability to obtain essentially non-oscillatory shock transitions.

Step 3. Compute the smoothness indicators β_r, $r = 0,1,2$ which measure how smooth the functions $P_r(x)$ are in the target cells $[x_j, x_{j+1}]$. The smaller these smoothness indicators, the smoother the functions are in different target cells. For the given values $f(u_i)$ with $x_i \in T_r$, the smoothness on T_r is estimated by employing the νth-order generalized undivided difference [9] which is defined as

$$D^{\nu}_r f(u_{j+\frac{1}{2}}) = \sum_{x_i \in T_r} a^{[\nu]}_{r,i} f(u_{j+i}), \tag{13}$$

for $\nu = 1,2$. The coefficient vector $\mathbf{a}^{[\nu]}_r := (a^{[\nu]}_{r,i} : x_i \in T_r)$ is calculated by solving the linear system

$$\sum_{x_i \in T_r} a^{[\nu]}_{r,i} \frac{(x_i - x_{j+\frac{1}{2}})^m}{m!} = \begin{cases} \Delta x^{\nu}, & \nu = m \\ 0, & \nu \neq m, \end{cases} \tag{14}$$

with $m = 0, \ldots, n_r - 1$ where n_r is the cardinality of T_r (for more details see [9]). More precisely, the functionals $D_r^1 f(u_{j+\frac{1}{2}})$ and $D_r^2 f(u_{j+\frac{1}{2}})$ with $r = 0, 1, 2$ can be written as

$$\begin{aligned}
D_0^1 f(u_{j+\frac{1}{2}}) &= -f(u_j) + f(u_{j+1}),\\
D_1^1 f(u_{j+\frac{1}{2}}) &= \frac{1}{24} f(u_{j-1}) - \frac{9}{8} f(u_j) + \frac{9}{8} f(u_{j+1}) - \frac{1}{24} f(u_{j+2}),\\
D_2^1 f(u_{j+\frac{1}{2}}) &= -f(u_j) + f(u_{j+1}),\\
D_0^2 f(u_{j+\frac{1}{2}}) &= f(u_{j-1}) - 2f(u_j) + f(u_{j+1}),\\
D_1^2 f(u_{j+\frac{1}{2}}) &= \frac{1}{2} f(u_{j-1}) - \frac{1}{2} f(u_j) - \frac{1}{2} f(u_{j+1}) + \frac{1}{2} f(u_{j+2}),\\
D_2^2 f(u_{j+\frac{1}{2}}) &= f(u_j) - 2f(u_{j+1}) + f(u_{j+2}).
\end{aligned} \tag{15}$$

In [8], it is demonstrated that

$$D_r^\nu f(u_{j+\frac{1}{2}}) = \frac{\mathrm{d}^\nu}{\mathrm{d}x^\nu} f(u_{j+\frac{1}{2}}) \Delta x^\nu + \mathscr{O}(\Delta x^3), \tag{16}$$

as can be verified by the Taylor expansion. The new smoothness indicators are proposed by

$$\beta_r = \left| D_r^1 f(u_{j+\frac{1}{2}}) \right| + \left| D_r^2 f(u_{j+\frac{1}{2}}) \right|, \quad r = 0, 1, 2. \tag{17}$$

The Taylor expansion at $x_{j+\frac{1}{2}}$ of those smoothness indicators yields

$$\begin{aligned}
\beta_0 &= \left| f'(u_{j+\frac{1}{2}}) \Delta x + \frac{1}{24} f^{(3)}(u_{j+\frac{1}{2}}) \Delta x^3 \right| + \left| f''(u_{j+\frac{1}{2}}) \Delta x^2 - \frac{1}{2} f^{(3)}(u_{j+\frac{1}{2}}) \Delta x^3 \right| + \mathscr{O}(\Delta x^4),\\
\beta_1 &= \left| f'(u_{j+\frac{1}{2}}) \Delta x - \frac{3}{640} f^{(5)}(u_{j+\frac{1}{2}}) \Delta x^5 \right| + \left| f''(u_{j+\frac{1}{2}}) \Delta x^2 + \frac{5}{24} f^{(4)}(u_{j+\frac{1}{2}}) \Delta x^4 \right| + \mathscr{O}(\Delta x^6),\\
\beta_2 &= \left| f'(u_{j+\frac{1}{2}}) \Delta x + \frac{1}{24} f^{(3)}(u_{j+\frac{1}{2}}) \Delta x^3 \right| + \left| f''(u_{j+\frac{1}{2}}) \Delta x^2 + \frac{1}{2} f^{(3)}(u_{j+\frac{1}{2}}) \Delta x^3 \right| + \mathscr{O}(\Delta x^4).
\end{aligned} \tag{18}$$

Step 4. Compute the non-linear weights based on the ideal weights and the smoothness indicators. Then, the non-linear weights are defined by

$$w_r = \frac{\alpha_r}{\sum_{l=0}^{2} \alpha_l}, \quad \alpha_r = d_r \left(1 + \left(\frac{\tau_4}{\beta_r + \varepsilon} \right)^2 \right), \quad r = 0, 1, 2, \tag{19}$$

with $\varepsilon = 10^{-12}$. Here, $\tau_4 = |\beta_2 - \beta_0|$ is the global smoothness indicator on the stencil T_1.

Step 5. The final reconstruction formulation of the numerical flux, defined by a convex combination of the three reconstructed polynomial approximations, is given by

$$\hat{f}_{j+\frac{1}{2}} = \frac{w_1}{d_1} \left[\hat{f}_{j+\frac{1}{2}}^{(1)} - d_0 \hat{f}_{j+\frac{1}{2}}^{(0)} - d_2 \hat{f}_{j+\frac{1}{2}}^{(2)} \right] + w_0 \hat{f}_{j+\frac{1}{2}}^{(0)} + w_2 \hat{f}_{j+\frac{1}{2}}^{(2)}. \tag{20}$$

Step 6. After doing the spatial discretization, a classical non-linear ODE system is generated as follows

$$\begin{aligned}\frac{\mathrm{d}u_j(t)}{\mathrm{d}t} =& \frac{1}{\Gamma(2-\alpha)}\Bigg(c_1\big(\frac{x_j-a}{2}\big)^{2-\alpha}\int_{-1}^{1} v\big(\frac{a+x_j}{2}+\frac{x_j-a}{2}\eta,t\big)(1-\eta)^{1-\alpha}\mathrm{d}\eta \\ &+ c_2\big(\frac{b-x_j}{2}\big)^{2-\alpha}\int_{-1}^{1} v\big(\frac{b+x_j}{2}+\frac{b-x_j}{2}\eta,t\big)(1+\eta)^{1-\alpha}\mathrm{d}\eta\Bigg)+f(x_j,t), \\ v_j(t) =& \frac{\hat{f}_{j+\frac{1}{2}}-\hat{f}_{j-\frac{1}{2}}}{\Delta x^2}.\end{aligned} \tag{21}$$

Then, the third-order version TVD Runge-Kutta time discretization scheme is employed to obtain fully discrete scheme both in space and time as follows [19]

$$\begin{aligned} u_j^{(1)} &= u_j^n + \Delta t F(u_j^n), \\ u_j^{(2)} &= \tfrac{3}{4}u_j^n + \tfrac{1}{4}u_j^{(1)} + \tfrac{1}{4}\Delta t F(u_j^{(1)}), \\ u_j^{n+1} &= \tfrac{1}{3}u_j^n + \tfrac{2}{3}u_j^{(2)} + \tfrac{2}{3}\Delta t F(u_j^{(2)}), \end{aligned} \tag{22}$$

where $F(u)$ is the spatial operator.

Remark 1. *As is said, the Gauss-Jacobi quadratures are employed for the two weakly singular integrals, but they usually cannot be guaranteed that all Gaussian nodes are the subsets of the points $\{x_j\}$. Accordingly, the interpolation is needed to obtain the values of the intermediate functions $v(x,t)$ at different Gaussian quadrature points. The degree of the interpolation polynomial is suitably considered such that the error caused in this approximation is of the same order as the error of the corresponding WENO-Z scheme.*

2.1 Analysis of the accuracy of WENO-Z scheme

Evaluating the polynomials $P_0(x), P_1(x)$ and $P_2(x)$ at $x = x_{j+\frac{1}{2}}$ and from (8) it can be seen that

$$\begin{aligned} \hat{f}^{(0)}_{j+\frac{1}{2}} = \hat{f}^{(2)}_{j+\frac{1}{2}} &= f(u_{j+1}) - f(u_j) = \int_{x_{j+\frac{1}{2}}}^{x_{j+\frac{3}{2}}}\int_{\chi-\frac{\Delta x}{2}}^{\chi+\frac{\Delta x}{2}} h(\psi)\mathrm{d}\psi\mathrm{d}\chi - \int_{x_{j-\frac{1}{2}}}^{x_{j+\frac{1}{2}}}\int_{\chi-\frac{\Delta x}{2}}^{\chi+\frac{\Delta x}{2}} h(\psi)\mathrm{d}\psi\mathrm{d}\chi, \\ \frac{1}{d_1}\big[\hat{f}^{(1)}_{j+\frac{1}{2}} - d_0\hat{f}^{(0)}_{j+\frac{1}{2}} - d_2\hat{f}^{(2)}_{j+\frac{1}{2}}\big] &= \frac{1}{12d_1}f(u_{j-1}) + C_d\big(f(u_j)-f(u_{j+1})\big) - \frac{1}{12d_1}f(u_{j+2}) \\ &= \frac{1}{12d_1}\int_{x_{j-\frac{3}{2}}}^{x_{j-\frac{1}{2}}}\int_{\chi-\frac{\Delta x}{2}}^{\chi+\frac{\Delta x}{2}} h(\psi)\mathrm{d}\psi\mathrm{d}\chi + C_d\int_{x_{j-\frac{1}{2}}}^{x_{j+\frac{1}{2}}}\int_{\chi-\frac{\Delta x}{2}}^{\chi+\frac{\Delta x}{2}} h(\psi)\mathrm{d}\psi\mathrm{d}\chi \\ &\quad - C_d\int_{x_{j+\frac{1}{2}}}^{x_{j+\frac{3}{2}}}\int_{\chi-\frac{\Delta x}{2}}^{\chi+\frac{\Delta x}{2}} h(\psi)\mathrm{d}\psi\mathrm{d}\chi - \frac{1}{12d_1}\int_{x_{j+\frac{3}{2}}}^{x_{j+\frac{5}{2}}}\int_{\chi-\frac{\Delta x}{2}}^{\chi+\frac{\Delta x}{2}} h(\psi)\mathrm{d}\psi\mathrm{d}\chi, \end{aligned} \tag{23}$$

where

$$C_d = -\frac{5}{4d_1} + \frac{d_0}{d_1} + \frac{d_2}{d_1}.$$

Now suppose the function $h(\psi)$ is smooth, so this function has Taylor expansion at point x_j, which is inserted into (23). By integrating, it can be seen that

$$\begin{aligned}
&\hat{f}^{(0)}_{j+\frac{1}{2}} = \sum_{\gamma=1}^{2} \frac{\Delta x^\gamma}{\gamma!} \frac{\mathrm{d}^\gamma h(x_j)}{\mathrm{d}x^\gamma} + \frac{1}{4} \frac{\mathrm{d}^3 h(x_j)}{\mathrm{d}x^3} \Delta x^3 + \mathscr{O}(\Delta x^4), \\
&\frac{1}{d_1}\left[\hat{f}^{(1)}_{j+\frac{1}{2}} - d_0 \hat{f}^{(0)}_{j+\frac{1}{2}} - d_2 \hat{f}^{(2)}_{j+\frac{1}{2}}\right] = \sum_{\gamma=1}^{2} \frac{\Delta x^\gamma}{\gamma!} \frac{\mathrm{d}^\gamma h(x_j)}{\mathrm{d}x^\gamma} - \frac{3d_0 + 3d_2 - 2}{12 d_1} \frac{\mathrm{d}^3 h(x_j)}{\mathrm{d}x^3} \Delta x^3 + \mathscr{O}(\Delta x^4), \\
&\hat{f}^{(2)}_{j+\frac{1}{2}} = \sum_{\gamma=1}^{2} \frac{\Delta x^\gamma}{\gamma!} \frac{\mathrm{d}^\gamma h(x_j)}{\mathrm{d}x^\gamma} + \frac{1}{4} \frac{\mathrm{d}^3 h(x_j)}{\mathrm{d}x^3} \Delta x^3 + \mathscr{O}(\Delta x^4).
\end{aligned} \tag{24}$$

Now, it can be seen that

$$g(x_{j+\frac{1}{2}}) = h(x_{j+1}) - h(x_j) = \sum_{\gamma=1}^{2} \frac{\Delta x^\gamma}{\gamma!} \frac{\mathrm{d}^\gamma h(x_j)}{\mathrm{d}x^\gamma} + \frac{1}{6} \frac{\mathrm{d}^3 h(x_j)}{\mathrm{d}x^3} \Delta x^3 + \mathscr{O}(\Delta x^4). \tag{25}$$

As mentioned above, to obtain the flux $\hat{f}^{(m)}_{i-\frac{1}{2}}$ it is only need to shift each index by -1. Therefore,

$$\begin{aligned}
&\hat{f}^{(0)}_{j\pm\frac{1}{2}} = g(x_{j\pm\frac{1}{2}}) + \frac{1}{12} \frac{\mathrm{d}^3 h(x_j)}{\mathrm{d}x^3} \Delta x^3 + \mathscr{O}(\Delta x^4), \\
&\frac{1}{d_1}\left[\hat{f}^{(1)}_{j\pm\frac{1}{2}} - d_0 \hat{f}^{(0)}_{j\pm\frac{1}{2}} - d_2 \hat{f}^{(2)}_{j\pm\frac{1}{2}}\right] = g(x_{i\pm\frac{1}{2}}) + \frac{d_1 - 1}{12 d_1} \frac{\mathrm{d}^3 h(x_j)}{\mathrm{d}x^3} \Delta x^3 + \mathscr{O}(\Delta x^4), \\
&\hat{f}^{(2)}_{j\pm\frac{1}{2}} = g(x_{j\pm\frac{1}{2}}) + \frac{1}{12} \frac{\mathrm{d}^3 h(x_j)}{\mathrm{d}x^3} \Delta x^3 + \mathscr{O}(\Delta x^4).
\end{aligned} \tag{26}$$

Proposition 1. *For the numerical flux $\hat{f}_{j+\frac{1}{2}}$ given by (20) that non-linear weights (19) is applied, the WENO-Z scheme can obtain the fourth-order accuracy in smooth areas.*

Proof. Adding and subtracting $d_0 \hat{f}^{(0)}_{j+\frac{1}{2}} + \left[\hat{f}^{(1)}_{j+\frac{1}{2}} - d_0 \hat{f}^{(0)}_{j+\frac{1}{2}} - d_2 \hat{f}^{(2)}_{j+\frac{1}{2}}\right] + d_2 \hat{f}^{(2)}_{j+\frac{1}{2}}$ from Eq. (20) gives

$$\begin{aligned}
\hat{f}_{j+\frac{1}{2}} &= \hat{f}^{(1)}_{j+\frac{1}{2}} + (w_0 - d_0)\hat{f}^{(0)}_{j+\frac{1}{2}} + (w_1 - d_1)\frac{1}{d_1}\left[\hat{f}^{(1)}_{j+\frac{1}{2}} - d_0 \hat{f}^{(0)}_{j+\frac{1}{2}} - d_2 \hat{f}^{(2)}_{j+\frac{1}{2}}\right] + (w_2 - d_2)\hat{f}^{(2)}_{j+\frac{1}{2}} \\
&= \left(g(x_{j+\frac{1}{2}}) - \frac{1}{90} \frac{\mathrm{d}^5 h(x_j)}{\mathrm{d}x^5} \Delta x^5 + \mathscr{O}(\Delta x^6)\right) \\
&\quad + \left((w_0 - d_0)\hat{f}^{(0)}_{j+\frac{1}{2}} + (w_1 - d_1)\frac{1}{d_1}\left[\hat{f}^{(1)}_{j+\frac{1}{2}} - d_0 \hat{f}^{(0)}_{j+\frac{1}{2}} - d_2 \hat{f}^{(2)}_{j+\frac{1}{2}}\right] + (w_2 - d_2)\hat{f}^{(2)}_{j+\frac{1}{2}}\right),
\end{aligned} \tag{27}$$

where the second parenthesis must be at least $\mathscr{O}(\Delta x^6)$ in smooth areas, in order to warranty the approximation to the second order derivative to be fourth-order accurate. Substituting Eq. (26), yields

$$\begin{aligned}
&(w_0 - d_0)\hat{f}^{(0)}_{j+\frac{1}{2}} + (w_1 - d_1)\frac{1}{d_1}\left[\hat{f}^{(1)}_{j+\frac{1}{2}} - d_0 \hat{f}^{(0)}_{j+\frac{1}{2}} - d_2 \hat{f}^{(2)}_{j+\frac{1}{2}}\right] + (w_2 - d_2)\hat{f}^{(2)}_{j+\frac{1}{2}} \\
&\qquad = -\frac{w_1 - d_1}{12 d_1} \frac{\mathrm{d}^3 h(x_j)}{\mathrm{d}x^3} \Delta x^3 + \sum_{r=0}^{2} (w_r - d_r)\mathscr{O}(\Delta x^4).
\end{aligned} \tag{28}$$

Notice that sum of d_r and sum of w_r with $r=0,1,2$ is one. The necessary and sufficient conditions are

$$\begin{cases} w_r - d_r \leq \mathscr{O}(\Delta x^2), & r=0,2, \\ w_1 - d_1 \leq \mathscr{O}(\Delta x^3). \end{cases} \tag{29}$$

From Eq. (18), one obtains $\tau_4 = \mathscr{O}(\Delta x^3)$. On condition that $\varepsilon << \beta_r$ with $r=0,1,2$ and considering (18) in smooth areas, it concludes

$$\left(\frac{\tau_4}{\varepsilon+\beta_r}\right)^2 = \mathscr{O}(\Delta x^4),$$

therefore

$$d_r = \frac{w_r}{1+\left(\frac{\tau_4}{\varepsilon+\beta_r}\right)^2} \sum_{l=0}^{2} \alpha_l = w_r + \mathscr{O}(\Delta x^4), \tag{30}$$

accordingly the conditions (29) satisfy and proof is completed. □

3 Computational results

In this section, some numerical experiments are considered to test the performance of the new fourth-order finite difference WENO scheme with Z-type non-linear weighting procedure. In order to check whether the random choice of the ideal weights would pollute the accuracy of the new WENO-Z scheme in smooth areas, three different types of the linear weights are tested in the numerical examples:
(1) $\gamma_0 = 0.05, \gamma_1 = 0.9, \gamma_2 = 0.05$;
(2) $\gamma_0 = \gamma_1 = \gamma_2 = \frac{1}{3}$;
(3) $\gamma_0 = 0.4, \gamma_1 = 0.2, \gamma_2 = 0.4$,
respectively.

Example 1. The fractional differential equation

$$\frac{\partial}{\partial t}u(x,t) = {}_0^cD_x^{1.8}u(x,t) + f(x,t), \tag{31}$$

with the initial condition $u(x,0) = \sin(4\pi x) - 2\sin(2\pi x)$ and periodic boundary conditions is solved. The computational domain is $[0,1]$. Its exact solution is $u(x,t) = \exp(-t)\big(\sin(4\pi x) - 2\sin(2\pi x)\big)$ and $f(x,t)$ is numerically obtained. The new WENO-Z scheme is employed and the errors and numerical orders of accuracy are reported in Table 1. As can be seen, the random selection of the ideal weights will not pollute the scheme's optimal order of accuracy in smooth areas.

Example 2. In this example, the fractional differential equation

$$u_t + Vu_x = D\nabla^\alpha u, \tag{32}$$

with the computational domain $[-L,L]$ is solved, where $2\nabla^\alpha u = {}_a^cD_x^\alpha u + {}_x^cD_b^\alpha u$, $V=0.5$, and $L=1$ or $L=10$.

In this test case, there is no exact solution, thus the approximate solution of 1000 grid points is considered as the exact solution, named as "Reference" solution. In Figs. 1, 2 and 3, the numerical solutions

Table 1: L_1 and L_∞ errors and the order of convergence for Example 1 at $T = 0.1$ with $\Delta t = 0.4\Delta x^2$.

	Case (1)				Case (2)			
N	L_∞-error	L_∞-order	L_1-error	L_1-order	L_∞-error	L_∞-order	L_1-error	L_1-order
10	1.76(-2)	-	7.84(-3)	-	1.90(-2)	-	7.24(-3)	-
20	1.29(-3)	3.77	4.51(-4)	4.12	1.23(-3)	3.95	4.00(-4)	4.26
40	7.42(-5)	4.12	2.70(-5)	4.06	9.08(-5)	3.77	2.70(-5)	5.06
80	4.26(-6)	4.12	1.90(-6)	3.83	4.63(-6)	4.29	1.62(-6)	4.88
160	2.77(-7)	3.95	1.23(-7)	3.95	2.77(-7)	4.06	1.01(-7)	5.12
320	1.52(-8)	4.18	7.67(-9)	4.01	1.87(-8)	3.89	7.08(-9)	5.17

	Case (3)			
N	L_∞-error	L_∞-order	L_1-error	L_1-order
10	1.90(-2)	-	6.95(-3)	-
20	1.39(-3)	3.77	4.16(-4)	4.06
40	7.72(-5)	4.18	2.93(-5)	3.83
80	4.82(-6)	4.00	1.83(-6)	4.00
160	2.88(-7)	4.06	1.34(-7)	3.77
320	1.59(-8)	4.18	7.68(-9)	4.12

and Reference solutions for different orders of the fractional derivative and different the linear weights are demonstrated at $T = 0.01$. As can be seen, there is no noticeable oscillations at the discontinuities. Also, it is verified that WENO-Z can generate similar numerical results with different types of the linear weights. In Fig. 1, the numerical solutions are demonstrated which obtained by employing the method in which the second spatial derivative is approximated by considering the second central difference method. It is obvious that the numerical solutions by the second central difference method demonstrate oscillatory behavior. The numerical solutions for $D = 0.2$ and $\alpha = 1.8$ at different final time are shown in Fig. 4. In the simulations, the parameters are chosen as: $L = 10, N = 200$ and $\Delta t = 0.4\Delta x^2$. The numerical solutions for $D = 0.02$ and $\alpha = 1.8$ at different final time are shown in Fig. 5. In the simulations, the parameters are chosen as: $L = 10, N = 200$ and $\Delta t = 0.3\Delta x^{1.8}$.

4 Conclusions

In this paper, a numerical scheme for solving fractional differential equations with piecewise smooth solutions is discussed. First, the fractional derivative is split into a classical second derivative and a weakly singular integral. By developing a fourth-order WENO-Z scheme, the second derivative is approximated while the weakly singular integral is approximated by Gauss-Jacobi quadrature. Finally, a classical ODE system is obtained, which it is computed by the TVD Runge-Kutta scheme. Numerical examples demonstrate a fact that the proposed WENO-Z scheme can obtain high-order accuracy in smooth areas and suppress non-physical oscillations near strong discontinuities.

Acknowledgements

The author is very thankful to the reviewers for carefully reading the paper, their comments and suggestions have improved the quality of the paper.

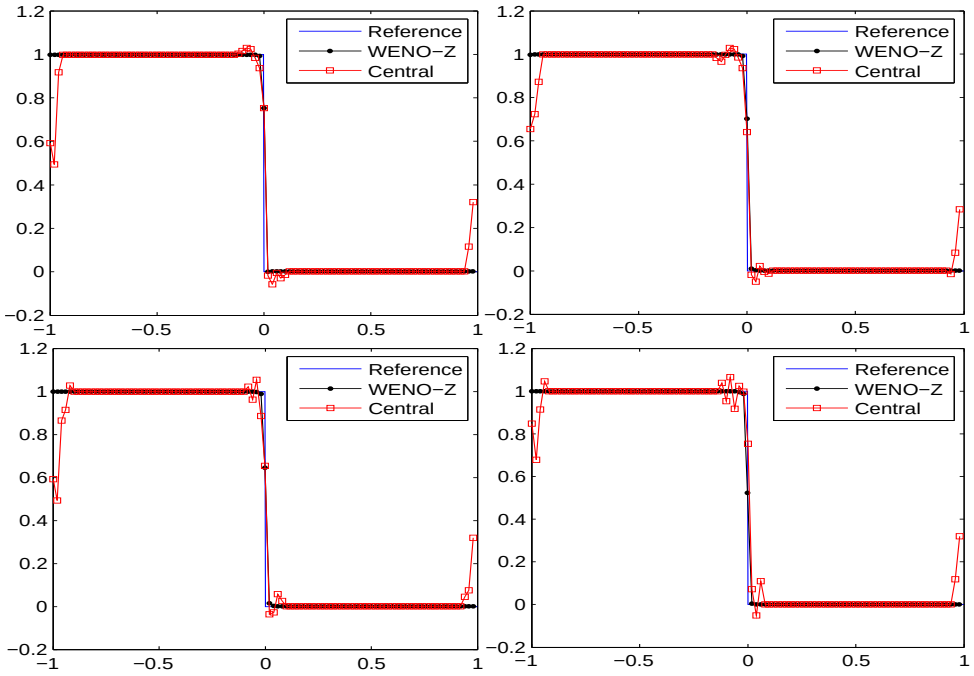

Figure 1: The numerical solutions of Example 2 with the linear weights (1) for different orders of the fractional derivative at $T = 0.01$. Top (left) to bottom (right): $\alpha = 1.2, 1.4, 1.6$ and $\alpha = 1.8$.

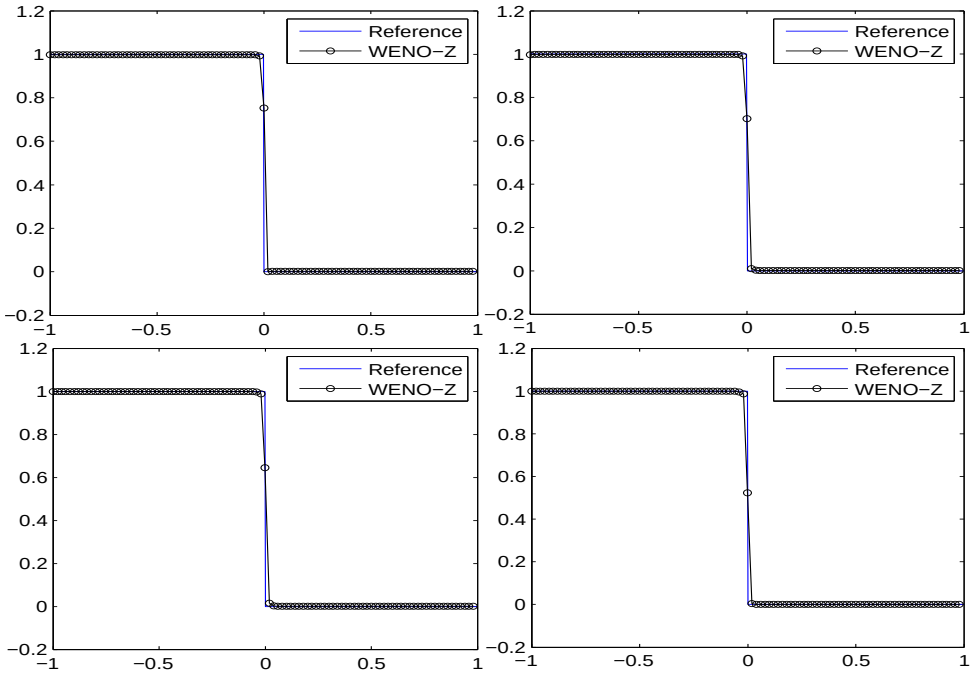

Figure 2: The numerical solutions of Example 2 with the linear weights (2) for different orders of the fractional derivative at $T = 0.01$. Top (left) to bottom (right): $\alpha = 1.2, 1.4, 1.6$ and $\alpha = 1.8$.

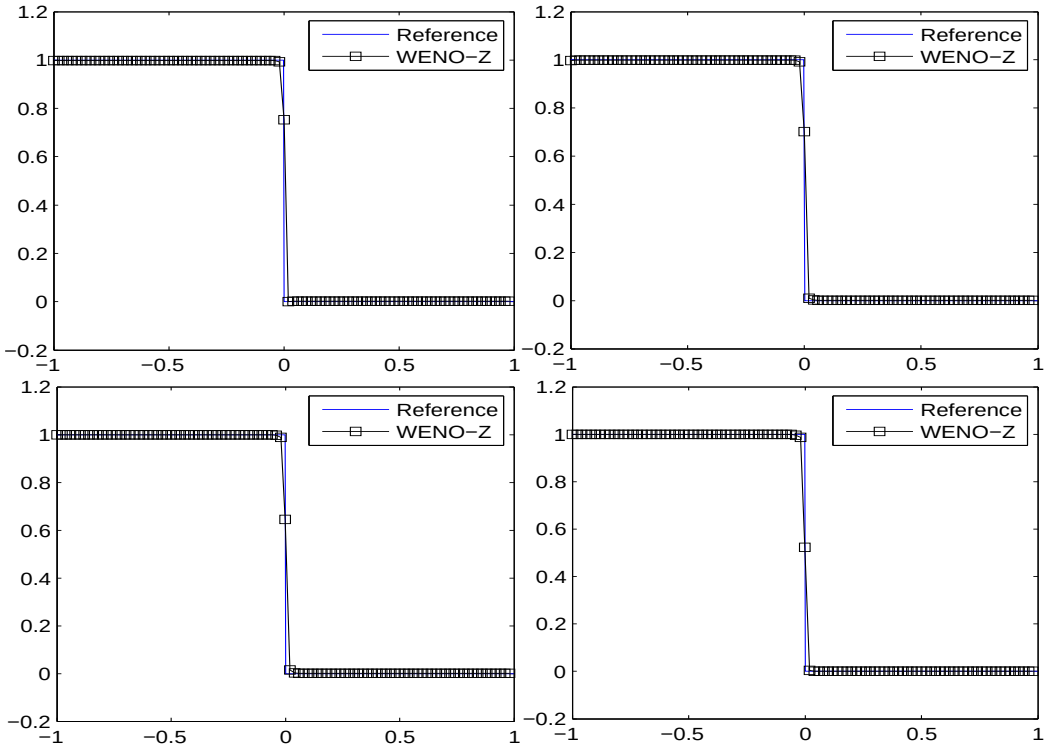

Figure 3: The numerical solutions of Example 2 with the linear weights (3) for different orders of the fractional derivative at $T = 0.01$. Top (left) to bottom (right): $\alpha = 1.2, 1.4, 1.6$ and $\alpha = 1.8$.

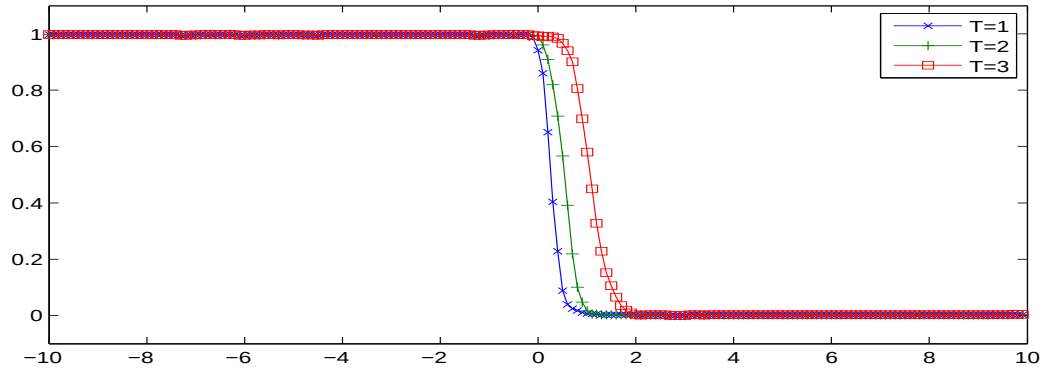

Figure 4: The numerical solutions of Example 2 with WENO-Z along with the linear weights (1). $\Delta t = 0.4\Delta x^2, \alpha = 1.8$ and $D = 0.2$.

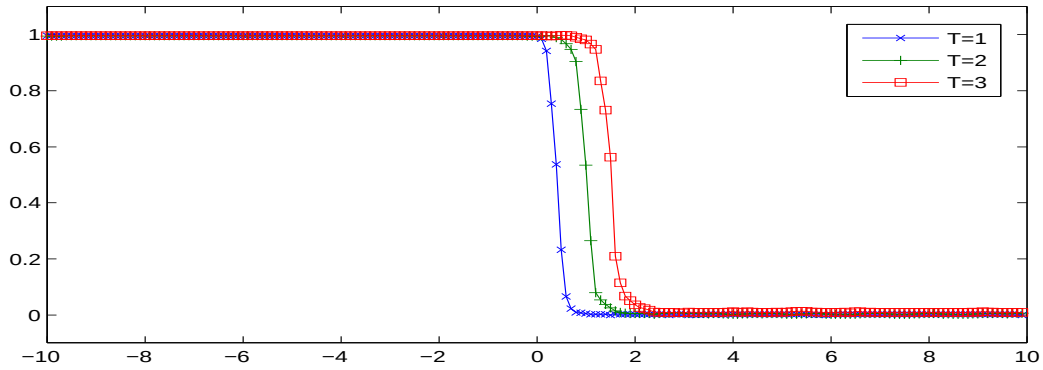

Figure 5: The numerical solutions of Example 2 with WENO-Z along with the linear weights (1). $\Delta t = 0.3\Delta x^{1.8}$, $\alpha = 1.8$ and $D = 0.02$.

References

[1] R. Abedian, *WENO schemes for multidimensional nonlinear degenerate parabolic pdes*, Iran. J. Numer. Anal. Optim. **8** (2018) 41–62.

[2] R. Abedian, *A new high-order weighted essentially non-oscillatory scheme for non-linear degenerate parabolic equations*, Numer. Methods Partial Differ. Equ. **37** (2021) 1317–1343.

[3] R. Abedian, *WENO-Z schemes with Legendre basis for non-linear degenerate parabolic equations*, Iran. J. Math. Sci. Inform. **16** (2021) 125–143.

[4] R. Abedian, H. Adibi, M. Dehghan, *A high-order weighted essentially non-oscillatory (WENO) finite difference scheme for nonlinear degenerate parabolic equations*, Comput. Phys. Commun. **184** (2013) 1874–1888.

[5] R. Abedian, M. Dehghan, *A high-order weighted essentially nonoscillatory scheme based on exponential polynomials for nonlinear degenerate parabolic equations*, Numer. Methods Partial Differ. Equ. **38** (2022) 970–996.

[6] W.H. Deng, *Finite element method for the space and time fractional Fokker-Planck equation*, SIAM J. Numer. Anal. **47** (2008) 204–226.

[7] W.H. Deng, S.D. Du, Y.J. Wu, *High order finite difference WENO schemes for fractional differential equations*, Appl. Math. Lett. **26** (2013) 362–366.

[8] Y. Ha, C. Kim, H. Yang, J. Yoon, *Sixth-order weighted essentially nonoscillatory schemes based on exponential polynomials*, SIAM J. Sci. Comput. **38** (2016) A1984–A2017.

[9] Y. Ha, C.H. Kim, Y.J. Lee, J. Yoon, *An improved weighted essentially non-oscillatory scheme with a new smoothness indicator*, J. Comput. Phys. **232** (2013) 68–86.

[10] A. Harten, B. Engquist, S. Osher, S. Chakravarthy, *Uniformly high-order essentially non-oscillatory schemes, III*, J. Comput. Phys. **71** (1987) 231–303.

[11] G.-S. Jiang, C.-W. Shu, *Efficient implementation of weighted ENO schemes*, J. Comput. Phys. **126** (1996) 202–228.

[12] X.J. Li, C.J. Xu, *Existence and uniqueness of the weak solution of the space-time fractional diffusion equation and a spectral method approximation*, Comput. Phys. Commun. **8** (2010) 1016–1051.

[13] F. Liu, V. Anh, I. Turner, *Numerical solution of the space fractional Fokker-Planck equation*, J. Comput. Appl. Math. **166** (2004) 209–219.

[14] X.-D. Liu, S. Osher, T. Chan, *Weighted essentially non-oscillatory schemes*, J. Comput. Phys. **115** (1994) 200–212.

[15] Y. Liu, C.-W. Shu, M. Zhang, *High order finite difference WENO schemes for nonlinear degenerate parabolic equations*, SIAM J. Sci. Comput. **33** (2011) 939–965.

[16] M.M. Meerschaert, C. Tadjeran, *Finite difference approximations for fractional advection-dispersion flow equations*, J. Comput. Appl. Math. **72** (2004) 65–77.

[17] I. Podlubny, Fractional differential equations, Academic Press, New York, 1999.

[18] J. Shi, C. Hu, C.-W. Shu, *A technique of treating negative weights in WENO schemes*, J. Comput. Phys. **175** (2002) 108–127.

[19] C.-W. Shu, S. Osher, *Efficient implementation of essentially non-oscillatory shock-capturing schemes*, J. Comput. Phys. **77** (1988) 439–471.

[20] C.-W. Shu, S. Osher, *Efficient implementation of essentially non-oscillatory shock-capturing schemes II*, J. Comput. Phys. **83** (1989) 32–78.

[21] Y. Zhang, W. Deng, J. Zhu, *A new sixth-order finite difference WENO scheme for fractional differential equations*, J. Sci. Comput. **87** (2021) 73.